energies

MDPI

Article

Investment Opportunities for Individual Energy Supply Systems: A UK Household Study

Julien Garcia Arenas [1,*], Mathieu Patin [2,3], Patrick Hendrick [1], Sylvie Bégot [2], Frédéric Gustin [2] and Valérie Lepiller [2]

[1] Department of Aero-Thermo-Mechanics, Université Libre de Bruxelles, F. D. Roosevelt Avenue 50, 1050 Brussels, Belgium
[2] Université de Franche-Comté, FEMTO-ST Laboratory (C.N.R.S.), 14 Rue des Entrepreneurs, 90000 Belfort, France; mathieu.patin@cea.fr (M.P.); frederic.gustin@univ-fcomte.fr (F.G.); valerie.lepiller@univ-fcomte.fr (V.L.)
[3] Université Grenoble Alpes, CEA, Liten, DTCH, 38000 Grenoble, France
* Correspondence: julien.garcia.arenas@ulb.be

Abstract

The current evolution of the energy context and progress in sustainable energy technologies are enabling the development of new energy supply systems for the residential sector. However, the techno-economic assessment of such energy systems is not straightforward and depends, among others, on the building type, its thermal insulation rate, and user patterns, as well as on the climatic conditions or energy and technology prices. This study therefore aims to develop an investment model for a typical UK household energy system that is applied to a diversity of scenarios to highlight the sensibility of the output results over stochastic input data such as electricity and heat demands, ambient temperature, and global solar irradiation. This dwelling diversity dataset is generated using a thermal–electrical demand model that uses stochastic techniques to model uncertainty. This contribution concludes with a discussion on how end-users can effectively take part in the energy transition while minimizing their energy bill and potentially generate long-term revenues. The main results show stable economic performance, with capital expenditure (CAPEX) ranging from GBP 15,400 to GBP 17,000 and NPV from GBP 21,000 to GBP 26,000 over 2000 individual scenarios. This study also confirms the leveraging effect of policy instruments, such as subsidies, in shifting the optimal system design towards higher shares of renewable and storage technologies, further reducing the reliance on fossil fuels and the impact on distribution systems.

Keywords: multi-energy systems; optimal design; households; load diversity; case study; stochastic dataset; policy

check for updates

Academic Editors: Fuzhan Nasiri, Ursula Eicker and Karthik Panchabikesan

Received: 10 July 2025
Revised: 16 October 2025
Accepted: 24 October 2025
Published: 4 November 2025

Citation: Garcia Arenas, J.; Patin, M.; Hendrick, P.; Bégot, S.; Gustin, F.; Lepiller, V. Investment Opportunities for Individual Energy Supply Systems: A UK Household Study. *Energies* **2025**, *18*, 5803. https://doi.org/10.3390/en18215803

Copyright: © 2025 by the authors. Licensee MDPI, Basel, Switzerland. This article is an open access article distributed under the terms and conditions of the Creative Commons Attribution (CC BY) license (https://creativecommons.org/licenses/by/4.0/).

1. Introduction

The current trend in European Union (EU) and United Kingdom (UK) energy policies is to ensure clean and affordable energy by increasing the share of renewable energy sources (RES) and reducing dependence on fossil fuels [1,2]. In the building sector, these strategies translate into improving energy performance through insulation measures, the use of efficient appliances, and the deployment of renewable technologies such as rooftop photovoltaics (PVs) and electric heat pumps (EHPs). Support schemes are also implemented to protect energy-poor households and mitigate the impact of the ongoing energy crisis on price volatility.

This large-scale transition towards modern home energy supply systems (HESSs), combined with decreasing technology costs and uncertain energy prices, is transforming end-users into potential investors in their own energy infrastructure. A typical household can now generate and store its own energy to reduce its energy bill and, in the long term, even generate income compared to conventional centralized supply systems.

However, assessing the techno-economic performance of such decentralized systems is complex. It often requires optimization models capable of determining the optimal design and operation of the system under given constraints. These models can address intermittency challenges and optimize energy flows over a defined period according to specific objectives, such as minimizing cost or carbon footprint [3]. However, achieving accurate and reliable results depends on several factors: a detailed representation of system components, a suitable spatio-temporal resolution, and a representative set of input data. Inevitably, a trade-off arises between model accuracy and computational complexity [4].

Adding to this challenge, modern energy systems are subject to multiple sources of uncertainty such as climate conditions, energy demands, renewable energy production, and commodity prices [5]. From a consumer-centered perspective, it becomes essential to identify which technology combinations are most profitable given local climatic, economic, and regulatory conditions. At the same time, uncertainty and diversity among households must be captured to provide representative investment insights.

Indeed, the energy demand of residential buildings depends on numerous factors: the type and size of the dwelling, its renovation status, the number of occupants, their behavior and comfort preferences, and their use of appliances. Each household has its own load profile, defining its specific energy needs throughout the day and year. Consequently, the design and operation of a HESS must be adapted to these unique characteristics. Using generic or aggregated consumption patterns as input for optimization models can therefore lead to inaccuracies in sizing or operating strategies [6].

Accurate input data is thus essential. This includes not only energy prices and technology costs but also realistic energy demand and renewable generation profiles. Two main approaches exist for generating these profiles. Top-down models rely on standardized load profiles (SLPs) derived from the aggregation of large numbers of households, offering simplicity but limited representativeness. In contrast, bottom-up models reconstruct energy consumption from individual behaviors, occupancy patterns, and appliance use. Though more complex and data-intensive, bottom-up approaches provide much greater flexibility and realism when capturing household diversity [7].

Furthermore, as the electrification of thermal energy needs through heat pumps increases, power and heat demand profiles become interdependent. Understanding and estimating space heating (SH) and domestic hot water (DHW) requirements therefore becomes as crucial as modeling electricity demand itself. Consequently, investment and optimization models must rely on multi-energy system (MES) frameworks to account for the interactions between different energy vectors and ensure a coherent, integrated representation of the household energy supply.

Although extensive research has been conducted on the optimal sizing and operation of residential PV-battery systems, most existing studies fail to capture these interdependencies between electricity and heat demands, or to adequately represent household diversity. Mulleriyawage et al. [8] reviewed the literature on residential PV-battery systems and concluded that optimal battery sizing mainly depends on the power load profile and the local tariff structure. They also highlighted a general lack of consideration for diversity in residential loads. Similarly, Deng et al. [9] proposed an advanced mathematical framework for optimal residential battery design, but their model did not include heat supply, nor did it account for diversity or uncertainty in the input data.

In contrast, using the energy hub (EH) concept, Kaffash et al. [10] developed a mathematical framework for the optimal scheduling of a battery within a PV–battery–heat pump system. However, their analysis did not consider thermal storage and assumed perfect knowledge of PV production and building consumption, limiting the realism of the operational results. Mittelviefhaus et al. [11] extended this line of research by jointly optimizing e-mobility and MES under uncertainty, yet their model also excluded thermal energy storage (TES) and did not integrate dwelling diversity in the uncertainty analysis.

Similarly, Nicoletti et al. [12] performed a cost-optimal sizing study for a comparable system but without considering TES or climatic uncertainty. Their analysis also focused exclusively on five warm Mediterranean locations, which limits the applicability of the results to colder climates. Nordgård-Hansen et al. [13] examined the optimal design and operation of a detached house energy system (solar, battery, and ground-source heat pump) in Norway, yet they also neglected TES and did not use individual energy demand profiles, opting instead for "low," "normal," and "high" consumption scenarios.

Further methodological advances have been made in modeling the operation of storage systems. Baniasadi et al. [14] developed a sophisticated framework for the optimal design and operation of thermal and electrical energy storage systems in a smart building, incorporating elements of model predictive control (MPC) to manage energy flows. However, their work remained limited to storage sizing and considered only a restricted number of scenarios. Schwarz et al. [15] proposed a stochastic program for a MES similar to the one analyzed in this study, accounting for different pricing mechanisms and weather-related uncertainties. Nevertheless, their analysis relied on standardized load profiles aggregated over 29 households, preventing detailed insights at the individual dwelling scale.

Building on these findings and addressing the identified research gaps, the present work focuses on the optimal sizing of a residential PV–battery–EHP–TES system for a single detached UK dwelling. Particular attention is paid to incorporating uncertainty in climate conditions and diversity in household energy use. The goal is to produce results that are representative of the UK building stock, thus supporting decision-making for consumers and policymakers investing in modern home energy supply systems.

The case study is based on 2000 simulated scenarios capturing variations in consumption and production profiles representative of different UK households and weather years. The optimization outputs include the optimal sizing of technologies, the quarterly operation of energy generation and storage units, their contribution to the overall energy supply, and key economic indicators such as investment cost, operating cost, and net present value (NPV) over the project lifetime.

The multi-energy system integrates three energy vectors—electricity, natural gas, and heat—and three supply sources: grid electricity, natural gas, and on-site PV generation. It comprises two conversion technologies (an air-to-water electric heat pump and a residential gas boiler) and two storage technologies (a lithium-ion battery and a thermal buffer tank). The system meets three types of energy demand: electricity consumption, SH, and DHW.

Nevertheless, the present model operates under a deterministic planning horizon, which may limit the generalizability of the results. Perfect foresight of weather and demand conditions simplifies the computational process for long-term design optimization, but it can overestimate performance and distort system sizing compared to real-world conditions, where only limited foresight is available.

This limitation can be mitigated by introducing a rolling-horizon approach, which balances long-term and short-term decision-making. As shown by Cuisinier et al. [16], such an approach effectively reduces the bias of deterministic assumptions in complex heating systems with seasonal storage. Rolling-horizon optimization is a cornerstone of MPC, or receding-horizon control, and has already been successfully applied in residential contexts:

Saleem et al. [17] used stochastic MPC for a PV–battery–EV charger system, while Yoshida et al. [18] applied it to a residential fuel cell cogeneration system with TES.

2. Methodology

In this section, we will first introduce the structure of the investment model, with a view on the inputs and outputs of the model shown in Figure 1. Hence, the HESS under study will then be described with help of a schematic view of the energy vectors and their interaction with the technologies involved given in Figure 2.

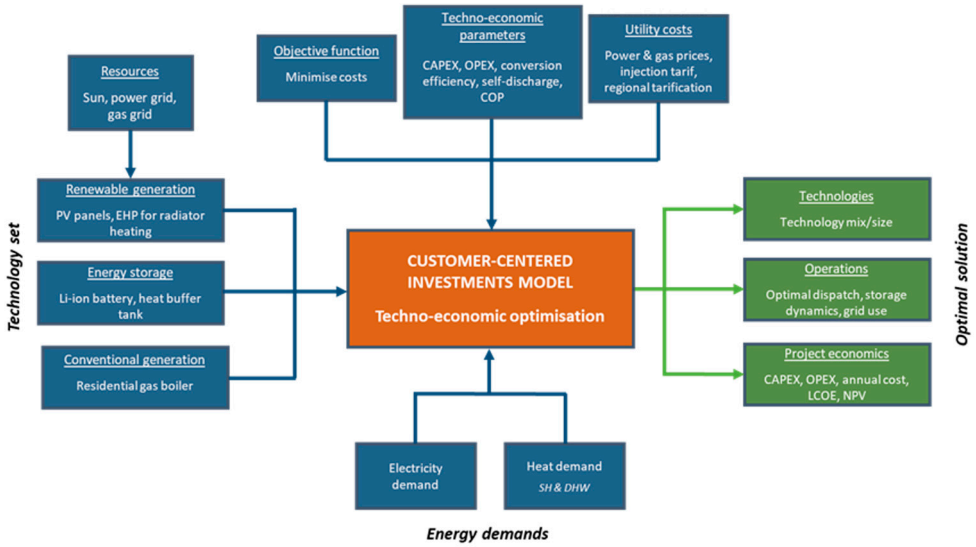

Figure 1. Schematic overview of the investment model's inputs and outputs [16].

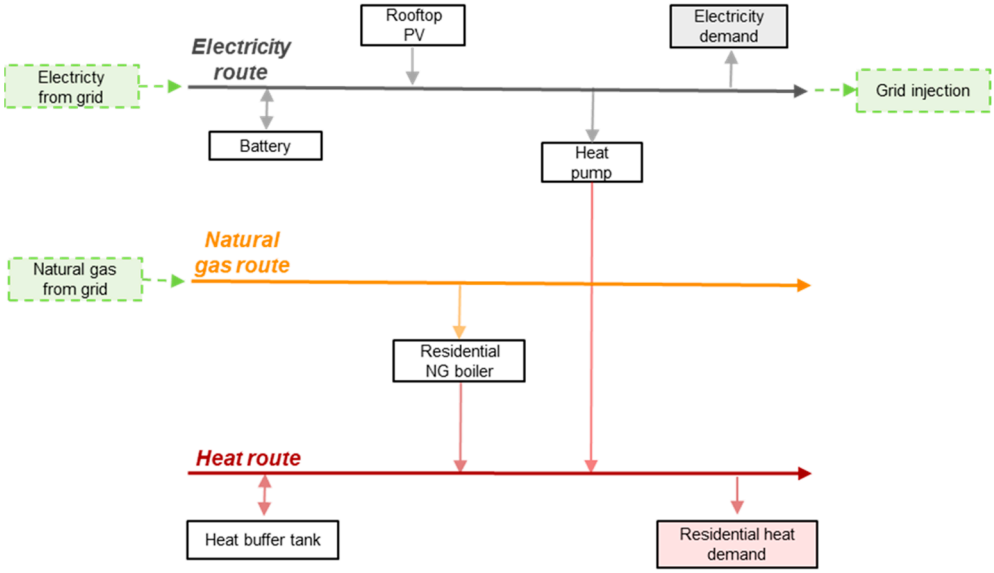

Figure 2. Schematic description of the home energy supply system under study.

As a second part, the modeling framework is provided with the presentation of the mathematical model. The model and its mathematical formulation are directly related to previous work [19,20] carried out as part of the *EPOC* project, granted by the Belgian Energy Transition Fund.

The third and last part of this section relates to the time series data process to generate dwelling diversity using stochastic techniques.

2.1. Description of the Investment Model

Figure 1 provides a schematic overview of the investment model structure. It illustrates input data, encompassing energy vectors, available production (renewable and conventional), and storage technologies, along with associated technical and economic parameters, system economics, energy demands, and the optimizer's objective function and model constraints.

The optimization yields outputs that include the selection and optimal sizing of technologies, the optimal operation of energy production and storage on a quarterly basis, the contribution of each unit to energy supply, and economic performance indicators, namely, investment and operating costs, as well as the net NPV at the end of project's lifetime.

The multi-energy system illustrated in Figure 2 involves three energy vectors (electricity, natural gas, heat) and three energy supply sources: grid-supplied electricity and natural gas, along with electricity generated by high-efficiency rooftop PV panels. The model incorporates two conversion technologies (air/water electric heat pump and a residential gas boiler) and two storage technologies (Li-ion battery and heat buffer tank). The energy requirements of the system include electricity consumption and SH and DHW demands.

The considered air-to-water EHP is for radiator heating purposes with an integrated DHW tank, providing heat for both SH and DHW demands. Equipped with DC inverter technology, the EHP is able to modulate its output heating power.

Complementing the EHP, a heat storage buffer tank can be installed to enhance the water volume in the radiator heating system. Acting like a thermal battery, it enables the heat pump to generate and store heat for subsequent use throughout the day. The heat buffer tank is also equipped with a spiral coil heat exchanger to facilitate the storage of domestic hot water along with space heating.

The decision-making of the optimizer for the dispatch of the energy flows is made according to the following choices [19]: At each time step, PV production is first used to meet the electricity demand. Any excess can be stored in the battery, injected to the grid, or converted into heat with the heat pump. This heat is then used directly to cover the thermal demand or stored in the buffer tank. If electricity demand remains, it is supplied by discharging the battery or importing from the grid. Likewise, any remaining heat demand is met either by the heat pump, using electricity from the battery or the grid, or by the existing gas boiler supplied with natural gas.

2.2. Mathematical Formulation

As mentioned above, the mathematical framework is related to previous work [19,20] and is formulated using Equations (1)–(12).

This investment model is a linear program designed for the economic dispatch of a residential energy supply system. The program utilizes input/output equations to represent the considered energy supply system. Over a year with an hourly time step i, this mathematical program optimizes energy flows based on predefined constraints and an objective function aimed at minimizing overall costs. Consequently, this program performs the long-term scheduling of the system presented in Figure 2, determining the optimal selection and sizing of technologies involved to achieve cost minimization. This model is deterministic and operates under the assumption of perfect forecasting of energy demands, production profiles of intermittent renewable technologies, and continuous availability of units throughout the year.

Four sets are introduced in the mathematical model: the simulation time interval I, containing the 8760 time steps of 1 h; the set of energy carriers E = {elec, CH4, heat}; the set of generating technologies G = {EHP, boiler}; and the set of storage technologies S = {battery, buffer tank}.

$$\forall\, i \in I, \forall\, e \in E, \forall\, g \in G, \forall\, s \in S,$$

$$minimise\Big(Obj = \Xi_{tot}^{annualised} + \Theta_{tot}\Big), \tag{1}$$

$$\Theta_{tot} = \sum^{t \in T} (\ FOM_t * K_t + VOM_t * \sum^{i \in I} P(i)_t^e * i) + C_{bill}, \tag{2}$$

$$\Xi_{tot}^{annualised} = \frac{D}{1-(1+D)^{-N}} * \sum^{t \in T} (capex_t * K_t), \tag{3}$$

$$P(i)_g^{e\prime} = \eta_g * P(i)_g^e, \tag{4}$$

$$SOC(i)_s = (1-\delta_s) * SOC(i-1)_s + i * (\eta_{s,\,c} * P(i)_{s,c} - \frac{P(i)_{s,d}}{\eta_{s,d}}), \tag{5}$$

$$P(i)_g^e \leq K_g, \tag{6}$$

$$P(i)_{s,c} \leq K_s^e, \tag{7}$$

$$P(i)_{s,d} \leq K_s^e, \tag{8}$$

$$SOC(i)_s \leq K_s^e, \tag{9}$$

The objective function defined in (1) aims to minimize the total annual costs of energy supply. This total cost is the sum of the annualized investment costs, $\Xi_{tot}^{annualised}$, and the total operating costs, Θ_{tot}, respectively, as described by (2) and (3). The annualization of investment costs is carried out over the project's economic lifetime N using the discount rate D. The total investment costs are calculated based on the installed capacities of the selected set of technologies T and their respective unit costs, while the total operating costs include both fixed and variable operation and maintenance expenses (FOM and VOM) for all technologies, as well as the annual energy bill C.

The conversion of one energy e vector into another e' is described by (4), where $P(i)_g^e$ is the power consumption of the carrier e required by the technology $g \in G$ to generate $P(i)_g^{e\prime}$, the equivalent power in terms of carrier e', with the conversion efficiency η_g.

The dynamics of the energy storage technology $s \in S$ are described in (5) with the update of the state-of-charge *SOC(i)* for each time-step, by considering $P(i)_{s,c}$ (resp., $P(i)_{s,c}$), the power flowing in (resp., out), and its associated charging efficiency $\eta_{s,\,c}$ (resp., discharging efficiency $\eta_{s,\,d}$). Energy losses via self-discharge of the storage technology from one time step to another are also accounted for in (5).

Moreover, (6) constrains the maximum power $P(i)_g^e$, with K_g corresponding to the installed capacity of the technology g. Similarly, in (7) and (8), the installed power capacity of the storage technology s, K_s^e constrains the charging power and discharging power of technology s. The installed energy capacity K_s^e in (9) finally sets a maximum value on the *SOC* of the storage technology s. We also deemed it realistic to constrain the installed capacities of PV and TES technologies with maximum values of 10 kWp and 35 kWh for a detached house, respectively, corresponding to a 22 m^2 surface area of PV panels and a 1000 L hot water tank with a 30 °C temperature elevation for storage.

Energy balance Equations (10)–(12) impose that, for each energy carrier, the amount of energy consumed or imported by the energy system at time-step i is at least equal to the amount of energy produced or exported.

$$\forall\, i \in I,$$

$$P(i)_{pv}^{elec} + P(i)_{bat,\,d}^{elec} + P(i)_{grid}^{elec} = P(i)_{demand}^{elec} + P(i)_{EHP}^{elec} + P(i)_{bat,c}^{elec} + P(i)_{injection}^{elec}, \tag{10}$$

$$P(i)_{boiler}^{heat} + P(i)_{EHP}^{heat} + P(i)_{buffer,d}^{heat} = P(i)_{demand}^{heat} + P(i)_{buffer,c}^{heat}, \tag{11}$$

$$P(i)_{grid}^{CH_4} = P(i)_{boiler}^{CH_4}, \quad (12)$$

The power balance Equation (10) requires that, at each time step, the total electricity supplied by rooftop PV, imported from the grid, and discharged from the battery is equal to the sum of direct electricity demand, the electricity consumed by the EHP, the electricity used for charging the battery, and the electricity exported to the grid. In parallel, the heat balance (11) ensures that the heat produced by the boiler, the electric heat pump, and the discharge from the thermal buffer tank matches the demand for SH and DHW or is stored in the buffer tank. Finally, Equation (12) specifies that the natural gas consumed by the back-up boiler must be equal to the amount imported from the gas grid.

2.3. Input Profiles Generation

To generate high-resolution profiles for domestic electricity and SH and DHW loads, along with global solar irradiation and ambient temperature profiles, we rely on the high-resolution stochastic integrated thermal–electrical domestic demand model [21] developed by the Centre for Renewable Energy Systems Technology (CREST). Their model uses statistics tools to stochastically generate behaviors (among others, occupancy, activities, heating, and cooling habits) and solicitation profiles (temperatures, solar radiation). These profiles are then used to generate domestic electricity, heating, and cooling demands [21–23]. The methodology is similar to the one developed in previous work [24] to generate an input dataset of 2000 scenarios, comprising time series for ambient temperature, global irradiation and rooftop PV production, electrical load, and SH and DHW demands with an hourly time step.

The CREST weather modeling includes two parts: radiation and ambient temperature modeling. For the radiation, the model first calculates the clear-sky solar radiation given the location and the day. Then, using a Markov chain, it estimates a clearness index profile representing the variation in the cloud cover throughout the day. Combining the clear-sky radiation with this profile gives the daily evolution of the solar radiation. For the temperature, the model picks, using an autoregressive moving-average model and weather data, a maximal and minimal temperature for the day. Then, using the daily variation in the solar radiation, it determines the temperature variation between those two values.

The electrical part of the CREST model first uses Markov chains to generate behavioral patterns (presence and sleep schedule) [22]. Then, it stochastically assigns to each dwelling a set of appliances based on national statistics. Finally, it generates the appliances' electricity profiles, combining these appliance sets with activity statistics, occupancy patterns, and appliances characteristics (mean power, mean running time…). For the lightning and hot water demand, the process is similar but also uses solar radiation for lighting. Figure 3 shows the type of electricity load profile that can be obtained with the CREST model (with a reduced number of appliances for visibility).

The thermal part of the CREST model, illustrated in Figure 4, is built around a grey-box building model, simulating variations in indoor temperature and, through heating control, determining the amount of heat required to maintain the desired temperature in the building.

The grey box model is composed of 3 capacities representing the thermal inertia of the building envelope, the indoor air, and the heating/cooling appliances, respectively. It also includes 3 heat transfer coefficients to represent the transfers from the ambient air to the building envelope, then to the indoor air, and finally, to/from the heating/cooling appliances. A fourth coefficient simulates losses associated with air movement. Four heat sources/sinks account for the exterior, the solar gains, the casual heat gains (inhabitants, appliances, lighting, and hot water tank losses), and heating.

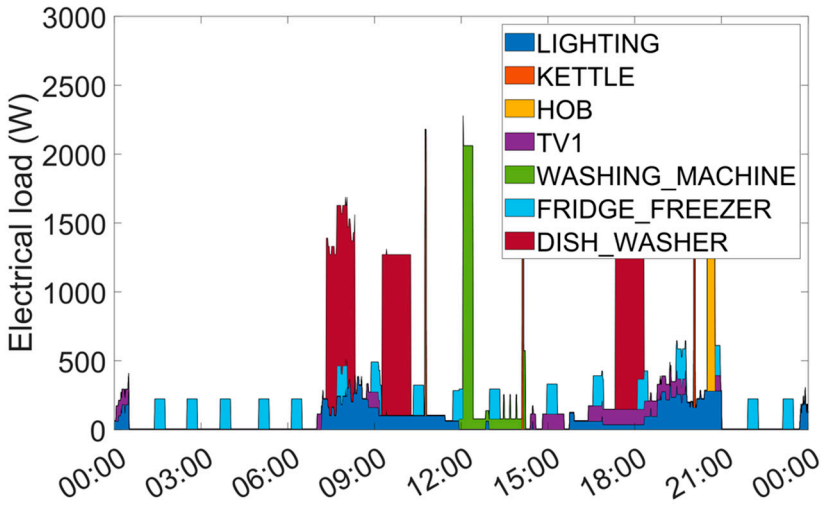

Figure 3. Electric load generated from the model with a few selected appliances.

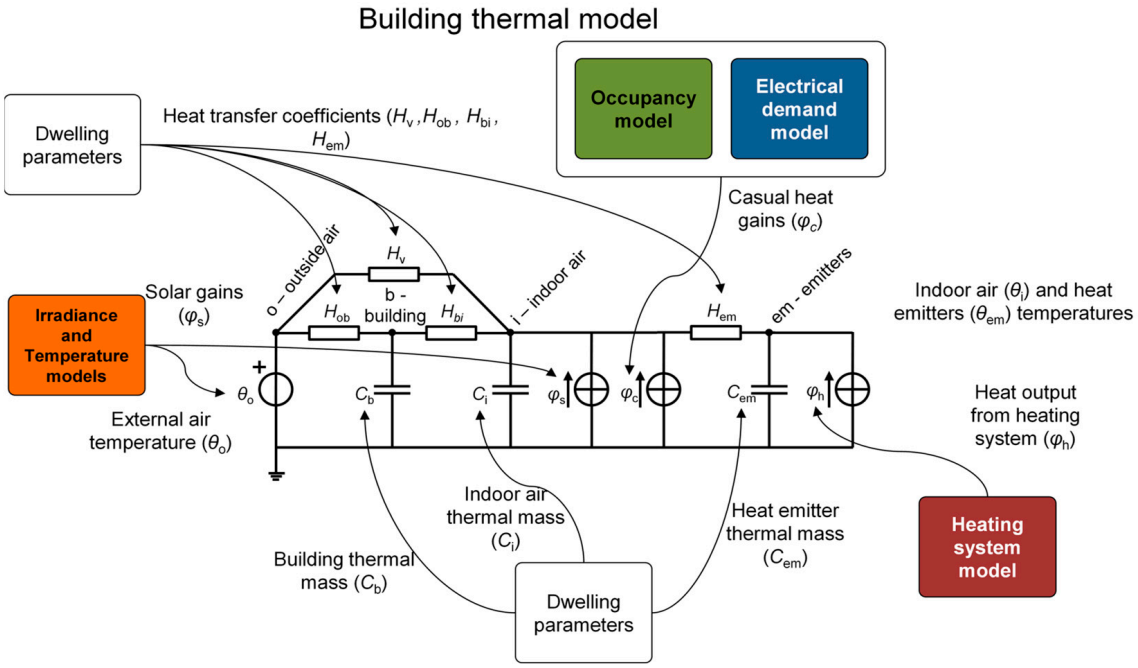

Figure 4. Thermal part of the CREST model [21].

Regarding heating control, the model's authors note that, due to limited data, simplifications were necessary [21]: heating setpoint temperatures were assigned to buildings stochastically, and the activation of the heating system is determined using transition probabilities, resulting in daily activation for an average of 10 h. However, this distribution is not linked to the occupancy patterns defined in the electrical load model and can therefore be inconsistent with them.

Finally, for hot water demand, the model applies a similar method to the electrical component: occupancy patterns and activity statistics are used to generate hot water demand profiles. The model then calculates the thermal demand associated with the amount of hot water drawn from the hot water cylinder and the temperature difference between the tank and the cold water inlet. The hot water thermal demand also includes static consumption to maintain the tank temperature at the setpoint.

To summarize, a list of all sources of variation in the domestic model can be found in Table 1.

Table 1. List of parameters used to generate diversity in load profiles.

Parameter	Parameter
Exterior temperature	Light bulbs ownership
Solar radiation	Bulbs switched on
Inhabitant number	Bulb cycle length
Inhabitant presence schedule	Hot water setpoint
Inhabitant sleep schedule	Hot water consumption
Appliances ownership	Space heating setpoint
Appliances switch on	Space heating schedule
Appliances cycle length	

The current CREST model iteration is available as an open-source Excel (version 16.82) spreadsheet [18]. It can be used to generate profiles that are high-resolution (one minute) and coherent with each other, meaning that a decrease in solar irradiation will simultaneously increase energy demand and decrease the PV production. However, the spreadsheet only allows for simulating one day at a time and is limited by Excel's computing speed.

To enable the generation of thousands of annual profiles, the model was reimplemented in the Matlab environment (version r2025a) and adapted to meet specific requirements of the present study. First, the gas boiler model was bypassed to obtain a generic heating demand rather than a gas-specific demand, allowing the heating load to be directly used as an input to the multi-energy system model. Second, the simulation is performed over a specified duration instead of a fixed 24 h period, which enables a more accurate analysis of continuous system behavior, mitigates the impact of initialization artifacts, and prevents abrupt shifts between consecutive days. Finally, the calculation of PV production is adjusted to account for the influence of PV module temperature on conversion efficiency.

3. Case Study

3.1. Description of the Case Study

The objective of the case study is to quantify the investment opportunities of a typical UK household for its energy supply considering uncertainty on climate data and diversity on power and heat profiles.

In this light, the techno-economic parameters adapted to the context of this case study are first presented in Tables 2 and 3, and a representative input dataset is then elaborated by generating 2000 individual energy demand profiles for electricity, SW, and DHW. This dataset is generated according to the parameters shown in Table 4 and presented in Figure 5.

Table 2 presents the investment and operation and maintenance (O&M) costs of the considered technologies, with the unit CAPEX parameters and the O&M parameters, divided into fixed (FOM) and variable (VOM) components for each technology involved in the model.

Table 2. Investment and operation and maintenance costs of involved technologies.

	CAPEX ($\frac{\textbf{GBP}}{\textbf{kW}}$)	**FOM** ($\frac{\textbf{GBP}}{\textbf{kW.y}}$)	**VOM** ($\frac{\textbf{GBP}}{\textbf{kWh.y}}$)
Rooftop PV	1372	9.1	0
Battery	515 *	0.46	1.85×10^{-3}
Heat pump	1110	12.63	0
Buffer tank	352	43 **	0.6×10^{-3}

* The unit CAPEX of the battery technology is the cost per installed kWh. ** The fixed annual cost of the buffer tank is the cost per unit installed.

Table 3 shows additional techno-economic parameters used for the analysis. The values of these parameters are determined according to technology catalogs [25–27] and the UK market consultation during spring 2024 for energy costs, feed-in tariffs, and grid fees.

Table 3. Other parameters of the case study.

Symbol	Description	Value
SC_{elec}	Standing charge for electricity supply (GBP/day)	0.534
SC_{NG}	Standing charge for natural gas supply (GBP/day)	0.298
c_{elec}^{peak}	Unit cost of electricity during peak hours (GBP/MWh)	335.98
$c_{elec}^{off\,peak}$	Unit cost of electricity during off-peak hours (GBP/MWh)	149.25
i_{elec}	SEG rate, feed-in tariff (GBP/MWh)	150
c_{NG}	Unit cost of natural gas (GBP/MWh)	74.2
η_{boiler}	Conversion efficiency of the NG condensing boiler (%)	97
η_{inv}	AC conversion efficiency of the PV inverter (%)	95
$\eta_{bat,c}$	Charging efficiency of the Li-ion battery (%)	98
$\eta_{bat,d}$	Discharging efficiency of the Li-ion battery (%)	97
δ_{bat}	Self-discharge rate of the Li-ion battery (%/h)	2.1×10^{-5}
δ_{tank}	Static leakage rate of the hot water buffer tank (%/h)	5×10^{-3}

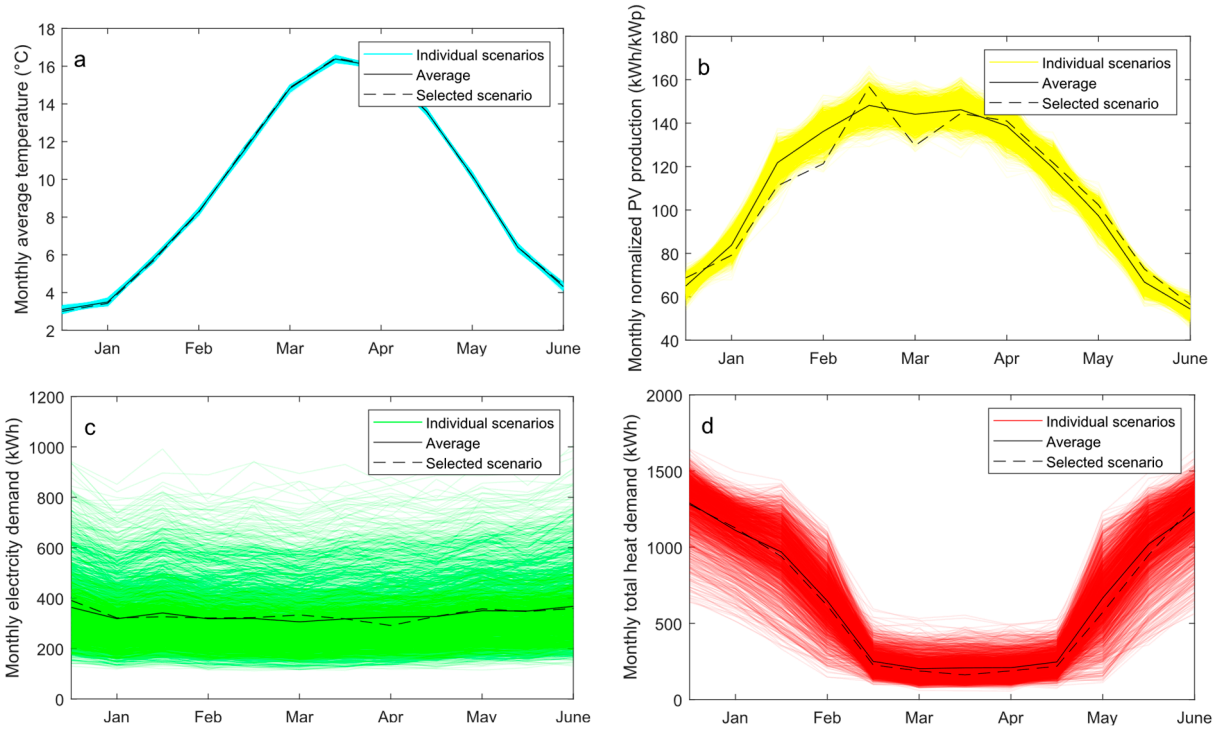

Figure 5. Representation of all individual profiles of the monthly (**a**) external ambient temperature; (**b**) PV production; (**c**) electricity demand; and (**d**) thermal load (space heating and domestic hot water). Average and selected profiles are also shown.

Note that the conversion efficiency of the heat pump technology η_{EHP} is referred to as the coefficient of performance (COP) and is computed for each time step according to the formulation from Runhau et al. [28] for radiator heating:

$$\forall\, i \in I,$$

$$\eta_{EHP} = COP(i) = 6.08 - 0.09 * \Delta T + 0.0005 * \Delta T^2, \tag{13}$$

$$\Delta T(i) = T^{sink}(i) - T^{source}(i), \tag{14}$$

$$T^{sink}(i) = 40\ ^{\circ}\mathrm{C} - 1.0 * T^{amb}(i), \quad (15)$$

$COP(i)$ is computed as a function of the temperature difference $\Delta T(i)$ between the heat sink and heat source temperatures, resp., $T^{sink}(i)$ and $T^{source}(i)$. External ambient air is the heat source for the air/water EHP, with $T^{source}(i) = T^{amb}(i)$.

Table 4. Parameters used to generate input profiles.

Parameter	Value
Simulation duration	365 days
Simulation starting day	January 1st
Location	Warwick, UK
Building type	Detached house
Insulation level	Improved CREST insulation
House area	136 m^2
Inhabitant number	1–5
Space heating setpoint	13–27 °C
Hot water setpoint	42–62 °C
PV efficiency	0.22
PV slope	40°
PV orientation	South
PV MPPE temperature coefficient	−0.38%/°C

3.2. Input Profiles Dataset

Following the methodology in Section 2.3, 2000 scenarios were generated for UK households based on the parameter values listed in Table 4. We defined a scenario as a subset of five stochastic profiles (i.e., ambient temperature, PV production, electrical load, and SH and DHW profiles) plus the COP time series that is derived for each time step i according to Equations (13)–(15).

The resulting scenarios are depicted in Figure 5, and their annual consumption is shown in Table 5 against 2022 UK averages [29] for a detached house (except for DHW, for which only EU averages [30] were found).

Table 5. Resulting average demand compared to UK average in 2022.

Results	Average Value	UK Average 2022 [26,27]
Electricity consumption	4001.7 kWh/y	4226 kWh/y
Hot water consumption	2503.6 kWh/y	2175 kWh/y
Space heating consumption	5545.9 kWh/y	15,104 kWh/y

Annual electricity and DHW consumption show deviations of −5.6% and +13.1%, respectively, compared to 2022 averages, which is deemed acceptable. However, SH consumption is significantly lower than the national average, reduced by a factor of 2.72. This discrepancy is likely to be attributed to the improved level of thermal insulation assumed in the building's thermal model, reflecting the rationale that improvements to the building envelope should precede investments in alternative home energy systems.

Additionally, two representative scenarios were created from the dataset using distinct methods. These scenarios, also presented in Figure 5, are used to compare the associated optimization results. The first "average scenario" was created by averaging the data from every profile at each time step. Then, the "selected scenario" was chosen as the most representative profile from the dataset of 2000 individual profiles. This selection process was based on a procedure developed by Sandia National Laboratories for generating Typical Meteorological Years (TMY) [31]. This method is based on the closeness between

the global Cumulative Distribution Function (CDF) of the daily values and each profile CDF. We evaluated the closeness for indices like exterior temperature, PV production, electricity load, and SH and DHW demand with an equal weight and selected profile number 617. While the weighting plays a role in the selection given the low likelihood for a single scenario to achieve the best statistics across all metrics, we deemed it sufficient to keep equal weights, since no indices were judged to be more important than others and satisfactory results were obtained.

Figures 5 and 6, respectively, show the monthly and daily behavior of scenario 617 against the overall average, highlighting stronger fluctuations due to the single-dwelling nature of the selected profile.

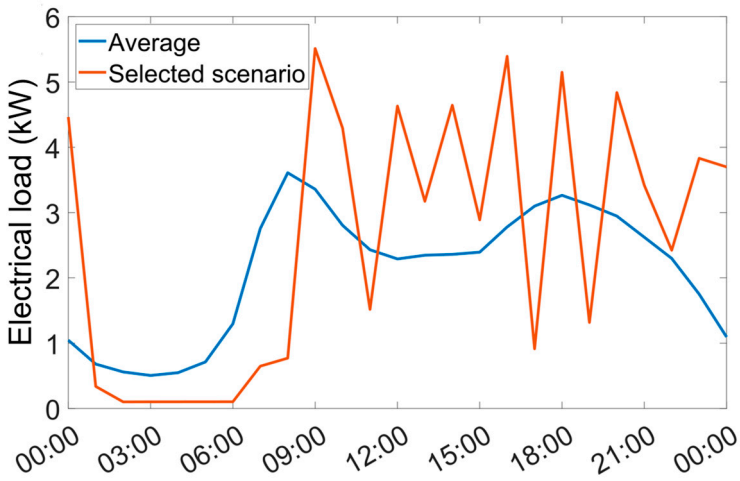

Figure 6. Comparison between the average electrical load and the selected profile 617.

4. Results and Discussion

For each scenario, the profitability of the investment opportunity is determined and compared against its reference for each individual scenario. The reference of the individual scenario consists of applying the same inputs to a simplified version of the investment model presented in Section 2.1, representing the business-as-usual (BAU) situation, i.e., only using electricity and natural gas from the grid to supply the energy needs. Consequently, the annual cash flows resulting from the cost differences between an individual scenario and its reference are used to compute the NPV of the project after 25 years.

Again, two additional designs are determined using the so-called average scenario and the selected scenario 617, represented in Figures 7 and 8, respectively, by a red cross and a green diamond. As explained in Section 3.2, the average scenario corresponds to a subset of the "averaged" profiles, with each profile resulting from the average of the 2000 individual profiles at every time step i. The selected profile 617 was selected as the most representative profile amongst the 2000 individual profiles according to the Sandia method based on CDF. These two scenarios are also used as inputs to the investment model, and the associated results are compared against the results of the 2000 individual scenarios.

To provide insights into the impact of policy decisions such as subsidies for renewable technologies or energy efficiency projects, this section concludes with a sensitivity analysis on system design and economic indicators for a progressive reduction in the investment costs.

In Figure 7, the four plots Figure 7a–d illustrate, respectively, the sizing of the rooftop PV, battery, EHP, and TES, while Figure 7e,f summarize the total initial investment and the NPV after 25 years. Figure 8 is used to present and compare the energy bills of the scenarios compared to their BAU counterpart: the two upper graphs in Figure 8a,b present the electricity and natural gas bills of the optimal designs, respectively, while

the bottom graphs Figure 8c,d show the electricity and natural gas bills of the reference scenarios, respectively.

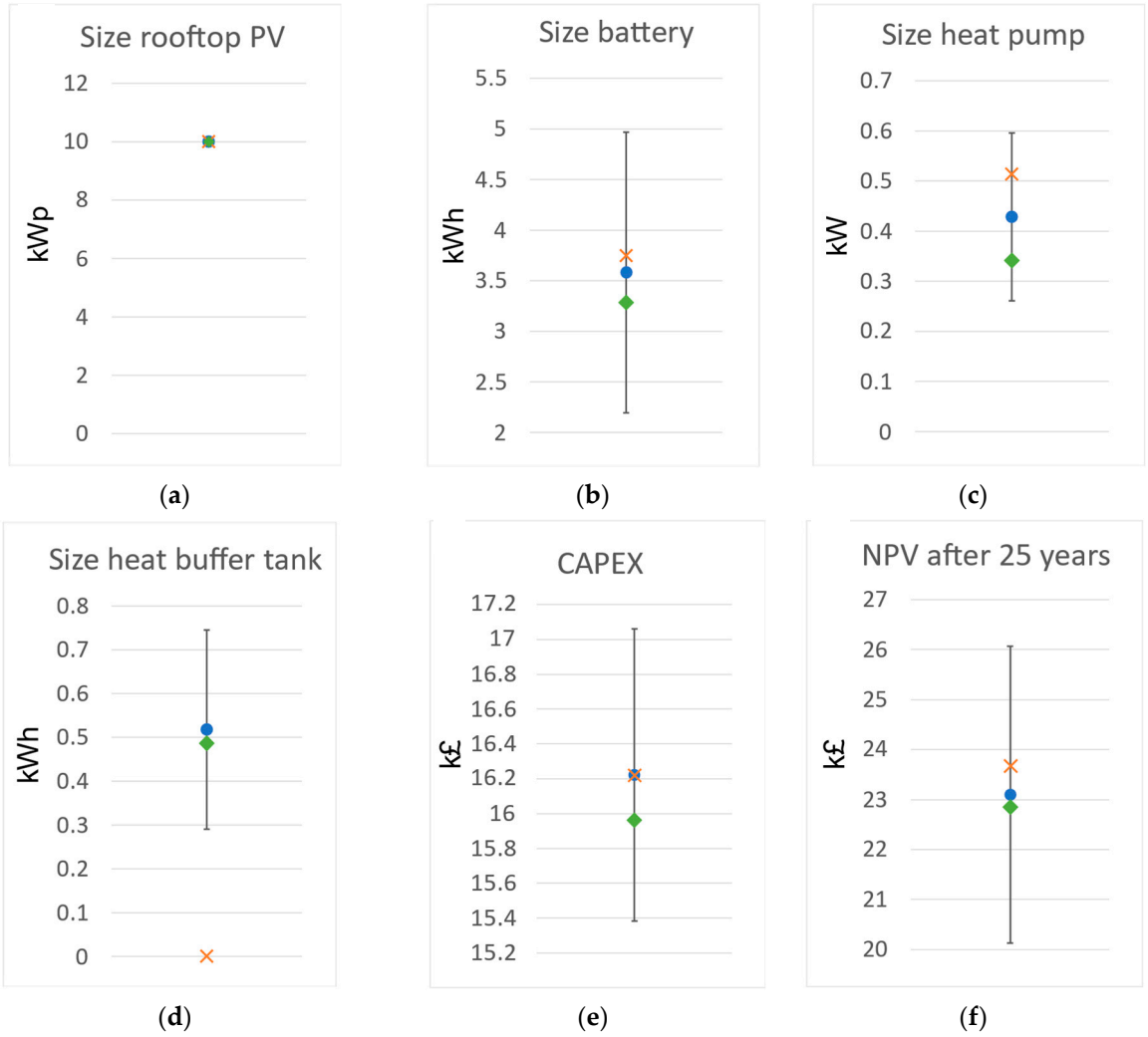

Figure 7. Output results of all scenarios from the case study: (**a**) rooftop PV sizing; (**b**) battery sizing; (**c**) heat pump sizing; (**d**) heat buffer tank sizing; (**e**) total CAPEX of the project; and (**f**) net present value after 25 years. The individual results are presented with error bars indicating the mean (blue dot) and standard deviation of the 2000 individual profiles; the result of the average profile is shown as a red cross, while the selected profile 617 is highlighted with a green diamond.

The four plots Figure 7a–d on the sizing of the technologies show that the installed PV capacity is always maximized by the optimizer, and this is explained by the fact that the revenues generated by feed-in of PV surplus to the grid are substantial; however, the sizing of the power-to-heat and storage technologies consequently vary, mainly due to the diversity of energy demand profiles. We indeed observe the battery sizing varying between 2.2 kWh to 5 kWh, EHP size ranging from 0.27 kW to 0.6 kW, and TES sizes from 0.3 kWh to 0.75 kWh.

On the other hand, we observe in the CAPEX and NPV graphs in Figure 7e,f that the economic performances are not subject to important variations, with CAPEX values stabilized between GBP 15,400 and GBP 17,000 and NPV values between GBP 21,000 and GBP 26,000. We particularly observe that, despite a significant initial investment requirement, investing in a PV–battery–heat pump–buffer tank system proves profitable, yielding an NPV of around GBP 23,000 after 25 years. Also, comparing the energy bills, Figure 8a–d shows that natural gas is still largely preferred in the alternative energy system,

with only a small portion of natural gas consumption being converted into electricity through power-to-heat conversion. Interestingly, even with this electrification of energy demand, the electricity bill in Figure 8c drops substantially, by around GBP 1000, compared to the business-as-usual case in Figure 8d.

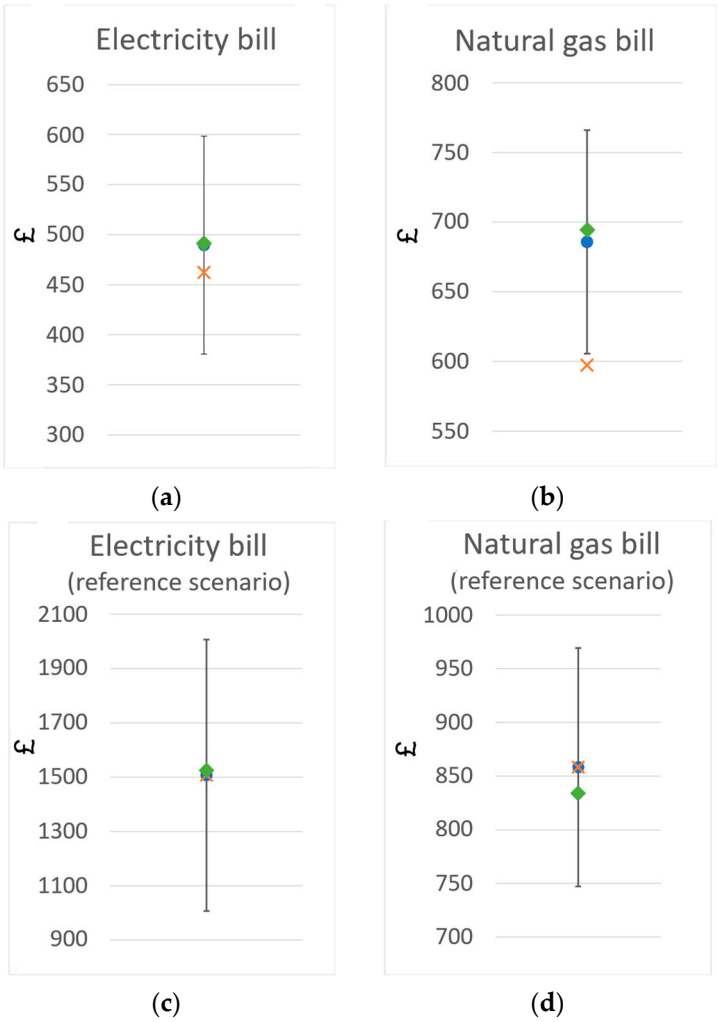

Figure 8. Output energy bills of the case study: (**a**) annual electricity bill; (**b**) annual natural gas bill; (**c**) annual electricity bill of the reference scenario; and (**d**) annual natural gas bill of the reference scenario. The individual results are presented with error bars indicating the mean (blue dot) and standard deviation of the 2000 individual profiles; the result of the average profile is shown as a red cross, while the selected profile 617 is highlighted with a green diamond.

Focusing on the results differences between the average of the 2000 individual scenarios, the average scenario, and the selected scenario 617, we observe that the output values of the selected scenario are closer to the average of the 2000 individual scenarios than ones of the average scenario are. This means that if we perform only one optimization using the selected scenario, the computational resources and associated solving time are divided by a factor 2000; employing the selected scenario therefore strikes a favorable balance between accuracy and computational efficiency.

It is also observed that the heat buffer tank capacity in Figure 7d is set to null by the optimizer when we consider the average scenario. The energy bills are also underestimated when using the average scenario, resulting in an overestimation of the NPV. Such discrepancies between the results of the average scenarios and the selected scenario can be explained

using Figure 6: we observe that the average profile is smoothened compared to the selected one, failing to capture the typical spikes observed in individual demand profiles.

Moreover, in view of the low values observed in Figure 7c,d for the sizing of EHP and buffer tank, it can be concluded that today, in the UK, installing an air-to-water EHP and a TES is not competitive compared to a natural gas boiler to supply heat in households; a small booster heat pump for hot water supply could be recommended instead.

Lastly, the sensitivity analysis in Figure 9 shows how system design and economic indicators evolve when the investment costs are progressively reduced in 10% steps. Scenario 617 is used as baseline scenario.

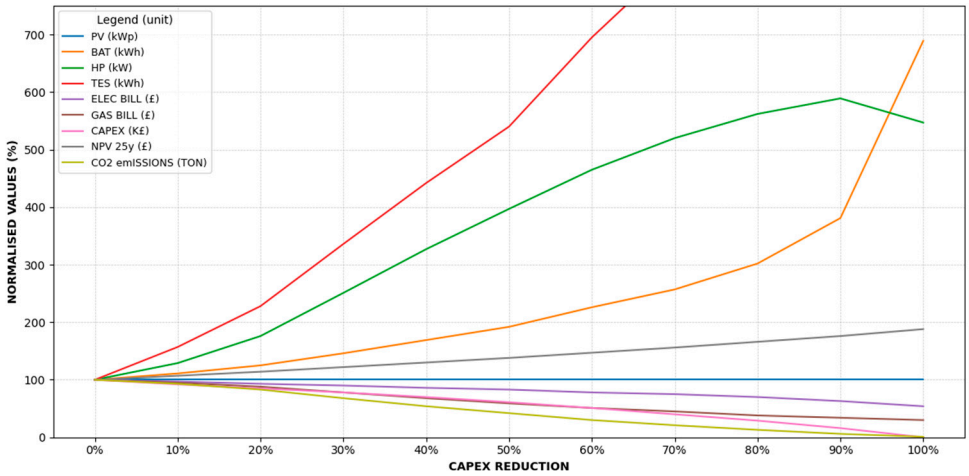

Figure 9. Evolution of indicators with CAPEX reduction, normalized to scenario 617's results.

For example, moving from 0% to a 50% CAPEX reduction, the thermal storage capacity increases from 0.5 MWh to more than 2.6 MWh (+420%) while battery storage grows from 3.3 kWh to over 6.3 kWh (+90%). In parallel, the heat pump capacity nearly quadruples, from 0.34 kW to 1.35 kW. These technological shifts are directly reflected in performance outcomes: as result of electrification of heat production, the gas bill reduces from GBP 694 to GBP 412 (−41%), and CO_2 emissions fall from 57.5 to 24.3 tons (−58%). The electricity bill decreases from GBP 491 to GBP 407 (−17%), surely due to the increase in electrochemical storage capacity. At the same time, the NPV over 25 years rises steadily from GBP 22.8k to GBP 31.6k, explained not only by the investment costs but also by the improved energy efficiency resulting from a greater use of PV energy. Indeed, the sensitivity analyses showed that revenues associated with feed-in of excess PV energy steadily decreased, favouring self-consumption to optimize energy bills. These trends are confirmed with the further decrease in CAPEX. It is interesting to note that the 100% reduction case represents the ideal design of the project, purely optimizing the operational costs of the energy system, initials costs aside. The results indicate a sudden decrease in HP capacity correlated to a significant increase in energy storage, with battery capacity almost doubling and TES capacity massively increasing up to the 35 kWh threshold that was set as the realistic maximum capacity for a home energy system. This suggests that storage capacities actually help to further cut carbon emissions to almost zero, but associated technology costs compared currently represent a barrier to zero-carbon buildings.

These results underline how the system design gradually transitions towards a higher penetration of renewable and flexible assets as investment costs decline, leading to simultaneous economic and environmental benefits. In this sense, policy instruments act as enablers for cost-effective decarbonization pathways by shifting the optimal system design towards higher shares of renewable and storage technologies while limiting carbon emissions and the impact on distribution systems.

5. Conclusions

This study presents a comprehensive methodology to assess investment opportunities in residential multi-energy systems, accounting for both climate variability and household demand diversity. A high-resolution bottom-up load profile generator, adapted from the CREST model, was implemented to generate a dataset of 2000 realistic UK household scenarios over a full year with an hourly resolution. These profiles capture the variability in electricity, space heating, domestic hot water demands, PV generation, and ambient temperature.

The investment model is formulated as a linear optimization problem that determines the optimal sizing of rooftop PV, battery storage, electric heat pump, and thermal buffer technologies while satisfying energy balances and technical constraints. Economic performance is evaluated over a 25-year horizon, including initial investments, operational costs, and revenues from grid injection.

The results show that while PV capacity is systematically maximized due to favorable tariffs, the optimal sizing of storage and power-to-heat technologies varies significantly depending on the scenario. However, the investment cost and net present value remain relatively stable, suggesting economic robustness. Importantly, the use of a single selected scenario, chosen via a CDF-based method, was proven to be effective in approximating a full stochastic analysis with reduced computational burden. In contrast, the average profiles tend to smooth-out variability, leading to biased sizing decisions and overestimated financial returns.

The findings further suggest that, in the UK context simulated in this work, gas boilers remain more economically attractive for space heating compared to electric heat pumps and thermal buffers, though the latter may still be relevant for domestic hot water.

Beyond the purely technical outcomes, the sensitivity analysis on initial costs demonstrates the importance of the broader policy and regulatory framework. Incentives such as subsidies for renewable installations, grants for energy efficiency projects, or dedicated reduced-interest loans can effectively lower financial barriers and drive the adoption of larger shares of storage and electrification technologies, which, in turn, can reduce households' energy bills, fossil fuel dependency, and carbon emissions. However, achieving net-zero energy buildings currently necessitates cost reductions that are not yet commercially viable.

This study ultimately highlights the leverage effect of political decisions: even modest policy incentives can significantly reshape the economic viability and configuration of decentralized multi-energy systems, accelerating the pathway towards low-carbon, resilient, and cost-effective energy solutions.

Author Contributions: Conceptualization, J.G.A. and M.P.; methodology, J.G.A.; software, J.G.A. and M.P.; validation, J.G.A. and M.P.; formal analysis, J.G.A. and M.P.; investigation, J.G.A. and M.P.; resources, J.G.A. and M.P.; data curation, J.G.A. and M.P.; writing—original draft preparation, J.G.A.; writing—review and editing, J.G.A.; visualization, J.G.A. and M.P.; supervision, P.H., S.B., F.G. and V.L.; project administration, P.H., S.B., F.G. and V.L.; funding acquisition, P.H., S.B., F.G. and V.L. All authors have read and agreed to the published version of the manuscript.

Funding: The work is supported via the energy transition funds project 'EPOC 2030–2050' organized by the FPS economy, S.M.E.s, Self-employed, and Energy.

Data Availability Statement: The original contributions presented in this study are included in the article. Further inquiries can be directed to the corresponding author.

Acknowledgments: Computations to generate input datasets have been performed on the supercomputer facilities of the Mésocentre de calcul de Franche-Comté.

Conflicts of Interest: The authors declare no conflicts of interest. The funders had no role in the design of the study; in the collection, analyses, or interpretation of data; in the writing of the manuscript; or in the decision to publish the result.

Abbreviations

The following abbreviations are used in this manuscript:

EU	European Union
UK	United Kingdom
RES	Renewable Energy Sources
PV	Photovoltaics
EHP	Electric Heat Pump
HESS	Home Energy Storage System
SLP	Synthetic Load Profile
SH	Space Heating
DHW	Domestic Hot Water
MES	Multi-Energy System
BESS	Battery Energy Storage System
EH	Energy Hub
TES	Thermal Energy Storage
NPV	Net Present Value
MPC	Model Predictive Control
CREST	Centre for Renewable Energy Systems Technology
CDF	Cumulative Distribution Function
O&M	Operation and Maintenance
CAPEX	Capital Expenditure
FOM	Fixed Operation and Maintenance
VOM	Variable Operation and Maintenance
COP	Coefficient Of Performance
BAU	Business-As-Usual

References

1. European Commission. RePowerEU: Joint European Action for More Affordable, Secure and Sustainable Energy. March 2022. Available online: https://eur-lex.europa.eu/legal-content/EN/TXT/PDF/?uri=CELEX:52022DC0108 (accessed on 23 October 2025).
2. HM Governement. British Energy Security Strategy: Secure, Clean and Affordable British Energy for the Long Term. April 2022. Available online: https://assets.publishing.service.gov.uk/media/626112c0e90e07168e3fdba3/british-energy-security-strategy-web-accessible.pdf (accessed on 23 October 2025).
3. Mancarella, P. Multi-energy systems: An overview of concepts and evaluation models. *Energy* **2014**, *65*, 1–17. [CrossRef]
4. Priesmann, J.; Nolting, L.; Praktiknjo, A. Are complex energy system models more accurate? An intra-model comparison of power system optimization models. *Appl. Energy* **2019**, *255*, 113783. [CrossRef]
5. Lasemi, M.A.; Arabkoohsar, A.; Hajizadeh, A.; Mohammadi-Ivatloo, B. A comprehensive review on optimization challenges of smart energy hubs under uncertainty factors. *Renew. Sustain. Energy Rev.* **2022**, *160*, 112320. [CrossRef]
6. Swan, L.G.; Ugursal, V.I. Modeling of end-use energy consumption in the residential sector: A review of modeling techniques. *Renew. Sustain. Energy Rev.* **2009**, *13*, 1819–1835. [CrossRef]
7. Pflugradt, N.; Teuscher, J.; Platzer, B.; Schufft, W. Analysing low-voltage grids using a behaviour-based load profile generator. In Proceedings of the ICREPQ'13, Bilbao, Spain, 20–22 March 2013. [CrossRef]
8. Mulleriyawage, U.G.K.; Shen, W.X. Impact of demand side management on optimal sizing of residential battery energy storage system. *Renew. Energy* **2021**, *172*, 1250–1266. [CrossRef]
9. Deng, X.; Wang, F.; Hu, B.; Lin, X.; Hu, X. Optimal sizing of residential battery energy storage systems for long-term operational planning. *J. Power Sources* **2022**, *551*, 232218. [CrossRef]
10. Kaffash, M.; Thoelen, K.; Deconinck, G. Optimal Scheduling of a Residential Energy Storage Device in Multi-Carrier Energy Systems. In Proceedings of the IEEE Benelux PELS/PES/IAS Young Researchers Symposium, Brussels, Belgium, 24–25 May 2018.

11. Mittelviefhaus, M.; Pareschi, G.; Allan, J.; Georges, G.; Boulouchos, K. Optimal investment and scheduling of residential multi-energy systems including electric mobility: A cost-effective approach to climate change mitigation. *Appl. Energy* **2021**, *301*, 117445. [CrossRef]
12. Nicoletti, F.; Cucumo, M.A.; Arcuri, N. Cost optimal sizing of photovoltaic-battery system and air–water heat pump in the Mediterranean area. *Energy Convers. Manag.* **2022**, *270*, 116274. [CrossRef]
13. Nordgård-Hansen, E.; Kishor, N.; Midttømme, K.; Risinggård, V.K.; Kocbach, J. Case study on optimal design and operation of detached house energy system: Solar, battery, and ground source heat pump. *Appl. Energy* **2022**, *308*, 118370. [CrossRef]
14. Baniasadi, A.; Habibi, D.; Al-Saedi, W.; Masoum, M.A.; Das, C.K.; Mousavi, N. Optimal sizing design and operation of electrical and thermal energy storage systems in smart buildings. *J. Energy Storage* **2020**, *28*, 101186. [CrossRef]
15. Schwarz, H.; Schermeyer, H.; Bertsch, V.; Fichtner, W. Self-consumption through power-to-heat and storage for enhanced PV integration in decentralised energy systems. *Sol. Energy* **2018**, *163*, 150–161. [CrossRef]
16. Cuisinier, É.; Lemaire, P.; Penz, B.; Ruby, A.; Bourasseau, C. New rolling horizon optimization approaches to balance short-term and long-term decisions: An application to energy planning. *Energy* **2022**, *245*, 122773. [CrossRef]
17. Saleem, M.I.; Saha, S.; Izhar, U.; Ang, L. A stochastic MPC-based energy management system for integrating solar PV, battery storage, and EV charging in residential complexes. *Energy Build.* **2024**, *325*, 114993. [CrossRef]
18. Yoshida, A.; Yoshikawa, J.; Fujimoto, Y.; Amano, Y.; Hayashi, Y. Stochastic receding horizon control minimizing mean-variance with demand forecasting for home EMSs. *Energy Build.* **2018**, *158*, 1632–1639. [CrossRef]
19. Arenas, J.G.; Hendrick, P. Task 3.3.2—Investment Opportunities for the Residential Consumer. September 2023. Available online: https://www.epocbelgium.be/sites/epoc/files/3.2.1%20Garcia%20Arenas%20ULB%20EPOC%20CONSUMER%20MODEL_1.6.pdf (accessed on 23 October 2025).
20. Arenas, J.G.; Hendrick, P.; Henneaux, P. Optimisation of Integrated Systems: The Potential of Power and Residential Heat Sectors Coupling in Decarbonisation Strategies. *Energies* **2022**, *15*, 2638. [CrossRef]
21. McKenna, E.; Thomson, M. High-resolution stochastic integrated thermal–electrical domestic demand model. *Appl. Energy* **2016**, *165*, 445–461. [CrossRef]
22. Richardson, I.; Thomson, M.; Infield, D. A high-resolution domestic building occupancy model for energy demand simulations. *Energy Build.* **2008**, *40*, 1560–1566. [CrossRef]
23. Richardson, I.; Thomson, M.; Infield, D.; Clifford, C. Domestic electricity use: A high-resolution energy demand model. *Energy Build.* **2010**, *42*, 1878–1887. [CrossRef]
24. Patin, M.; Bégot, S.; Gustin, F.; Lepiller, V. Comprehensive bottom-up methodology for generating high-resolution yearly building load profiles: A case study in temperate oceanic climate. *Energy Build.* **2024**, *320*, 114584. [CrossRef]
25. Danish Energy Agency, and Energinet. Technology Data: Generation of Electricity and District Heating. April 2020. Available online: https://ens.dk/sites/ens.dk/files/Statistik/technology_data_catalogue_for_el_and_dh_-_0009.pdf (accessed on 23 October 2025).
26. Danish Energy Agency, and Energinet. Technology Data: Heating Installations. June 2021. Available online: https://ens.dk/media/7372/download (accessed on 23 October 2025).
27. Danish Energy Agency, and Energinet. Technology Data: Energy Storage. January 2020. Available online: https://ens.dk/sites/ens.dk/files/Analyser/technology_data_catalogue_for_energy_storage.pdf (accessed on 23 October 2025).
28. Ruhnau, O.; Hirth, L.; Praktiknjo, A. Time series of heat demand and heat pump efficiency for energy system modelling. *Sci. Data* **2019**, *6*, 189. [CrossRef] [PubMed]
29. Department for Energy Security and Net Zero. National Energy Efficiency Data-Framework (NEED): Consumption Data Tables 2025—Headline Consumption Tables: England and Wales. 2023. Available online: https://assets.publishing.service.gov.uk/media/685bd3947d72089d199760d5/Consumption_headline_EW_2023.xlsx (accessed on 23 October 2025).
30. Odyssee-Mure Database. Sectoral Profile—Households—Energy Consumption by End-Use. Available online: https://www.odyssee-mure.eu/publications/efficiency-by-sector/households/household-eu.pdf (accessed on 23 October 2025).
31. Marion, W.; Urban, K. *User's Manual for TMY2s Typical Meteorological Years*; National Renewable Energy Laboratory: Golden, CO, USA, 1995. Available online: https://www.nrel.gov/docs/legosti/old/7668.pdf (accessed on 23 October 2025).

Disclaimer/Publisher's Note: The statements, opinions and data contained in all publications are solely those of the individual author(s) and contributor(s) and not of MDPI and/or the editor(s). MDPI and/or the editor(s) disclaim responsibility for any injury to people or property resulting from any ideas, methods, instructions or products referred to in the content.